ELSEVIER

1 November 1998

Optics Communications 156 (1998) 101–111

OPTICS COMMUNICATIONS

Full length article

On the VUV and UV $4f^7(^8S)5d \rightarrow 4f^8$ interconfigurational transitions of Tb^{3+} ions in $LiLuF_4$ single crystal hosts

E. Sarantopoulou [a,1], Z. Kollia [a], A.C. Cefalas [a,*], V.V. Semashko [b], R.Yu. Abdulsabirov [b], A.K. Naumov [b], S.L. Korableva [b]

[a] *National Hellenic Research Foundation, Theoretical and Physical Chemistry Institute, 48 Vassileos Constantinou Avenue, 116-35 Athens, Greece*

[b] *Kazan State University, 18 Lenin Street, 420008 Kazan, Russia*

Received 12 March 1998; revised 16 June 1998; accepted 1 July 1998

Abstract

The laser induced fluorescence spectrum of Tb^{3+} ions in $LiLuF_4$ single crystals, pumped by a fluorine pulsed discharge molecular laser at 157.6 nm, was obtained in the vacuum ultraviolet (VUV) and ultraviolet (UV) regions of the spectrum. The $4f^75d \rightarrow 4f^8$ dipole allowed transitions originate from the Stark components and the edge of the levels of the $4f^7(^8S)5d$ electronic configuration. The LIF spectra were interpreted on the basis of phonon trapping and phonon reabsorption within the levels of the $4f^75d$ electronic configuration. The absorption spectrum of the crystal samples in the VUV was obtained as well. We observed eight transitions between the ground level $4f^8(^7F_6)$ and the Stark components of the levels of the $4f^7(^8S)5d$ electronic configuration and five transitions between the ground level $4f^8(^7F_6)$ and the Stark components of the levels of the $4f^7(^6P)5d$ electronic configuration. The edge of the levels of the $4f^75d$ electronic configuration was found to be at $45.2 \times 10^3 \pm 0.2 \times 10^3$ cm^{-1} and the band gap of the crystal host was $77.6 \times 10^3 \pm 0.3 \times 10^3$ cm^{-1} wide.

1. Introduction

The vacuum ultraviolet (VUV) and ultraviolet (UV) absorption and emission spectroscopic characteristics of the rare earth (RE) ions, activated in the wide band gap of fluoride dielectric crystals, suggest that they can be used for a variety of applications, such as generation of laser light [1–3], light waveguides [4–6] and luminescence materials for new types of fluorescence bulbs [7,8]. The absorption and the emission spectra are mainly due to the transitions between the levels of the $4f^n$ electronic configuration and the levels of the $4f^{n-1}5d$ electronic configuration of the trivalent RE ions (where a 4f electron is promoted to a 5d localised band). These transitions, with strong Franck–Condon factors, are responsible for the broad band absorption and emission spectra. Because the energy levels of the $4f^{n-1}5d$ electronic configuration of the RE ions are situated 6–10 eV above the ground level of the $4f^n$ electronic configuration, various experimental methods have been applied for the excitation of the $4f^{n-1}5d$ electronic configuration, such as excitation with synchrotron and X-ray radiation sources [9,10] and multiphoton stepwise excitation [11,12]. In this paper, we report on the interconfigurational $4f^75d \rightarrow 4f^8$ VUV and UV fluorescence and absorption spectra of the Tb^{3+} ion in the $LiLuF_4$ single crystal host, as they are excited with laser radiation from the fluorine pulse discharge, molecular laser at 157.6 nm. This pumping arrangement populates the levels of the $4f^75d$ electronic configuration from the ground level of the RE trivalent ion, via one photon transition only. The subsequent deexcitation mechanism of the $4f^75d$

* Corresponding author. E-mail: ccefalas@eie.gr

[1] Permanent address: National Technical University of Athens, Physics Department Polytechnioupoli, Zografou, GR-15780 Athens, Greece.

0030-4018/98/$ - see front matter
PII: S0030-4018(98)00367-8

levels, efficiently populates the levels of the $4f^8$ electronic configuration of the Tb^{3+} ions. The absorption spectrum was also recorded at room and liquid nitrogen (LN_2) temperature, using a hydrogen lamp of stabilised longitudinal discharge. The absorption characteristics of the crystal samples in the VUV are due to the dipole transitions between the $4f^8$ ($^7F_6$) ground level of the RE trivalent ion, and the Stark components of the $4f^7$5d electronic configuration. The number and the spacing of the components depends on the site symmetry of the RE ion and the intensity of the crystal field. We observed eight dipole transitions between the $^7F_6$ ground level of the $4f^8$ electronic configuration and the Stark components of the levels of the $4f^7(^8S)$5d electronic configuration of the Tb^{3+} ion, and five transitions, between the $^7F_6$ ground level of the $4f^8$ electronic configuration and the Stark components of the levels of the $4f^7(^6P)$5d electronic configuration of the Tb^{3+} ion. Assignment to these transitions was made and the red limit (edge) of the levels of the $4f^7$5d electronic configuration was found to be (within the experimental error of 200 cm^{-1}) at 45.2×10^3 cm^{-1}. The energy levels in the spectral range from 80.0×10^3 to 71.4×10^3 cm^{-1} and from 71.4×10^3 to 45.2×10^3 cm^{-1} were assigned to the levels of the $4f^7(^6P)$5d and the $4f^7(^8S)$5d electronic configurations, respectively.

Furthermore, we report on the interconfigurational VUV and UV $4f^7$5d $\rightarrow 4f^8$ emission characteristics of the Tb^{3+} ions in $LiLuF_4$ single crystal hosts, as they are deexcited, following their excitation with the pulsed discharge fluorine molecular laser at 157.6 nm. The LIF spectrum can be explained provided that the $4f^7$5d $\rightarrow 4f^8$ dipole transitions originate from the Stark components Γ_1, $2\Gamma_2$, Γ_3, Γ_4, $3\Gamma_5$ of the $^2D_5$ level of the $4f^7(^8S)$5d electronic configuration. The emission from the Stark components is the result of phonon trapping and reabsorption, which is taking place between the levels of the $4f^7$5d electronic configuration. In the case of weak electron [$4f^{n-1}$]–phonon interaction [13–17], the phonon trapping and the reabsorption is a competitive process to the non-radiative relaxation within the levels of the $4f^n$5d electronic configuration.

2. Experimental

The LiLuF:Tb^{3+} monocrystals, were grown in carbon crucibles, with the Bridgman–Stockbarger method. The concentration of the Tb^{3+} ions in the samples was varied from 0.5 to 0.01 at%. The samples were optically polished disks, with diameter of 5 mm and their thickness was 0.5 mm. The experimental apparatus for obtaining the excitation spectrum consists of laser-pumping source, vacuum chamber where the crystal samples were placed, focusing optics and detection electronics. The laser pumping source was a laboratory build F_2 molecular laser described previously [19], it delivers 12 mJ per pulse and the pulse width was 12 ns at FWHM. The linewidth of the corresponding F_2 laser transition was found to be within the limit of the resolution of the monochromator of 0.1 nm, Fig. 1. The direction of the laser beam was parallel to the optical axis of the crystal and it was focused on the sample using a 60 cm concave mirror coated with MgF_2, at right angle to the laser axis. The fluorescence light was detected along the optical axis as well. In order to reduce the emission light from the laser discharge, a band-pass filter (23% transmis-

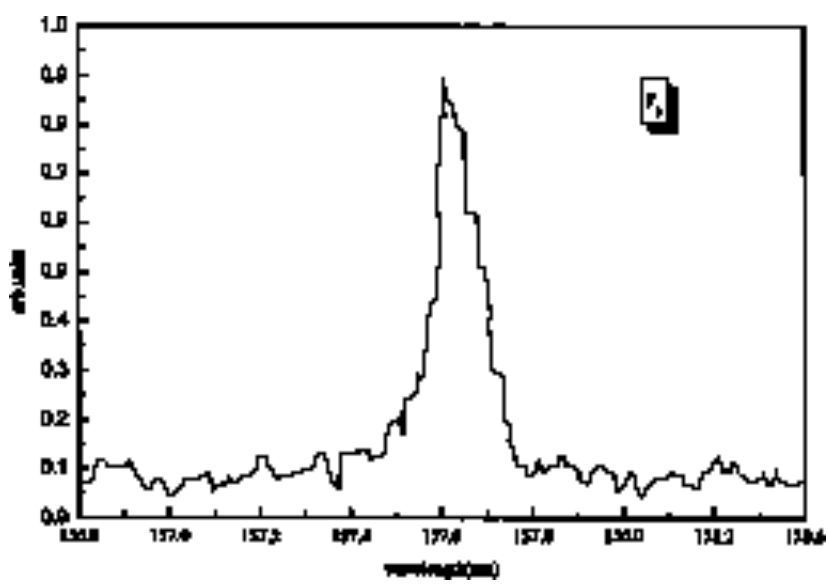

Fig. 1. Spectrum of the F_2 laser exciting pulse. The spectrum of the F_2 laser pulse at 157.6 nm shows the presence of two peaks at 157.6 and 157.5 nm. The peak at 157.5 nm is well supressed in a tuned cavity.

sion at 157.6 nm, 26 nm bandwidth) was placed in front of the crystal sample. We have used only 1 mJ to irradiate the crystal samples. The crystal sample was cooled down to liquid nitrogen temperature. The detection system consisted of a 0.2 m VUV monochromator (Acton VM502), a solar blind photomultiplier (EMI 9412) and a Box-Car integrator interfaced to a computer. The spectra were not deconvoluted with respect to the transfer function of the monochromator. The effect of the scattered light on the signal was reduced by placing the crystal sample inside a 5 cm long housing in such a way that no laser scattered light could enter the monochromator, except in the direction along the optical axis of the crystal. The absorption and the fluorescence spectra were detected with a resolution better than 0.5 nm. The optical path of the pumping laser beam, and the fluorescence signal, were kept within stainless steel vacuum lines at 10^{-5} mbar pressure.

3. Results and discussion

3.1. The absorption spectrum

The absorption spectrum of the trivalent Tb^{3+} ion has been studied previously in different crystal lattices [19–21]. The electric crystal field splits all the levels of the single and mixed configuration. The number and the spacing of the components depend on the symmetry and intensity of the crystal field. Such splitting has been observed previously for the Tb^{3+} ion in other dielectric crystal host materials as well. For example, regarding the $LiYF_4$:Tb^{3+} crystal (the site symmetry of the Tb^{3+} ion in the $LiYF_4$ and $LiLuF_4$ crystal hosts is C_{4h} or S_4 [22]), it was found that the electric crystal field splits the $4f^7$5d electronic configuration in five main Stark components with maximum absorption at 46.7×10^3, 51.5×10^3, 55.0×10^3, 60.6×10^3 and 80.9×10^3 cm^{-1}, respectively [18]. Similarly, for the LaF:Tb^{3+} crystal (C_2 or D_{3h} site symmetry) the electric crystal field splits the levels of the $4f^7$5d electronic configuration into nine main Stark components with maximum absorption at 54.0×10^3, 55.5×10^3, 57.8×10^3, 58.8×10^3, 61.3×10^3, 65.8×10^3 and 73.0×10^3 cm^{-1} respectively [19]. In the case of the free Tb^{3+} ion, Dieke and Crosswhite indicated that the $4f^7$5d electronic configuration splits into two groups of levels, and the energy gap between them extends from 55.7×10^3 to 65.0×10^3 cm^{-1} [23]. For the LaF_3 crystal, the edge of the levels of the $4f^2$5d configuration is at 50.0×10^3 cm^{-1} [19], for the CaF_2 crystal at 46.5×10^3 cm^{-1} [19] and around 44.9×10^3 cm^{-1} for the $LiYF_4$ crystal [18]. The edge of the levels of the $4f^7$5d electronic configuration in the case of the free Tb^{3+} ion is at 54.9×10^3 cm^{-1} [23].

According to Szczurek and Schlesinger [24], the $4f^7$ electronic configuration of the Tb^{3+} ion is half filled, and the lower energy level of the $4f^7$5d electronic configuration in this case is the $^8S_{7/2}$ one, which has zero total angular momentum. Therefore in a pure L–S coupling the 5d electron does not interact with the $4f^7$ shell, and the interaction is only through the crystal field. The 5d electronic configuration has two terms, the $^2D_{5/2}$ and the $^2D_{3/2}$ one, and they are split in three and two Stark components respectively in a crystal field of tetragonal symmetry ($^2D_{5/2} = 2\Gamma_7 + \Gamma_6$, $^2D_{3/2} = \Gamma_6 + \Gamma_7$). The situation for the $4f^7$5d electronic configuration is more complicated. There is a total number of 3106 levels of the $4f^7$5d electronic configuration. The $4f^7(^8S)$5d electronic configuration consists of two terms, the ^9D and the ^7D one, and only one of them, the $^7D_5$ is populated through the electric dipole transitions from the $4f^8(^7F_6)$ ground level of the $4f^8$ electronic configuration. At room temperature ($kT = 200$ cm^{-1}), the $4f^8 \rightarrow 4f^7$5d dipole transitions originate from the $4f^8(^7F_6)$ ground level, because the next excited level is the $^7F_5$ one, at 1.9×10^3 cm^{-1}. The crystal field of tetragonal symmetry should split the $^7D_5$ level into eight Stark components ($^7D_5 = \Gamma_1 + 2\Gamma_2 + \Gamma_3 + \Gamma_4 + 3\Gamma_5$).

3.1.1. 140–220 nm

The absorption spectrum was recorded with 0.01 at% concentration of Tb^{3+} ions and 0.5 mm thick crystal samples at liquid nitrogen temperature, Fig. 2. The absorption peaks were assigned to the $4f^8 \rightarrow 4f^7(^8S)$5d dipole transitions of the Tb^{3+} ion [24]. The absorption spectrum for 0.1 at% concentration of the RE ion and 0.5 mm thick crystal samples is shown in Fig. 3. Similarly the absorption spectrum for 0.5 at% concentration of the Tb^{3+} ion and 0.2 mm crystal thickness is shown in Fig. 4. The broadening of the Stark components and the shift of the absorption spectrum towards the red limit of the spectrum, with increased concentration of the Tb^{3+} ion, is due to the formation of Tb^{3+} ions of different site symmetry and clustering [24].

There were not significant differences between the absorption spectra taken at room and liquid nitrogen temperatures. The edge of the levels of the $4f^2$5d electronic configuration in the $LiLuF_4$ host was found to be at 45.2×10^3 cm^{-1} (within the accuracy of the experimental error of 200 wavenumbers). The eight Stark components of the $^7D_5$ level, were assigned to the levels of the $4f^7$5d electronic configuration at 47.0×10^3, 52.0×10^3, 54.4×10^3, 55.5×10^3, 55.9×10^3, 62.2×10^3, 64.3×10^3 and 67.5×10^3 cm^{-1} respectively. We exclude the formation of Tb^{3+} ions of different site symmetry, because at low concentration of the RE ion, only one type of optically active center is activated. In order to assign the theoretically expected eight Stark components of the $^7D_5$ level to the experimentally observed energy levels of the absorption spectrum, the exact solution of the secular equation should be known. However, to our knowledge, there are

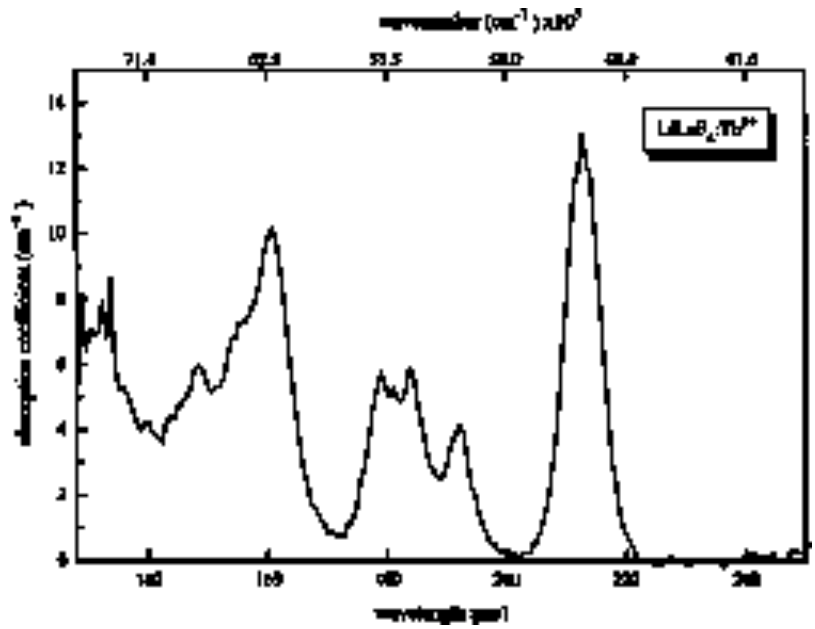

Fig. 2. Absorption spectrum of the $LiLuF_4:Tb^{3+}$ crystal in the spectral range from 125-300 nm. The concentration of the Tb^{3+} ion in the $LiLuF_4$ crystal was 0.01 at%, the crystal sample was 0.5 mm thick. The spectrum was recorded with resolution of 0.5 nm, and it was not corrected to the spectral response of the monochromator due to the fact that the linewidth difference between two electronic levels of the $4f^7 5d$ electronic configuration is larger than the resolution of the monochromator. The same applies for all the absorption and the LIF spectra.

no theoretical calculations regarding the energy position of the Stark components of the $^7D_5$ levels. The Stark components of the $4f^7 5d$ electronic configuration are represented by irreducible representations of the double cubic group (after their decomposition into irreducible representations of the S_4 or the C_{4u} double tetragonal group).

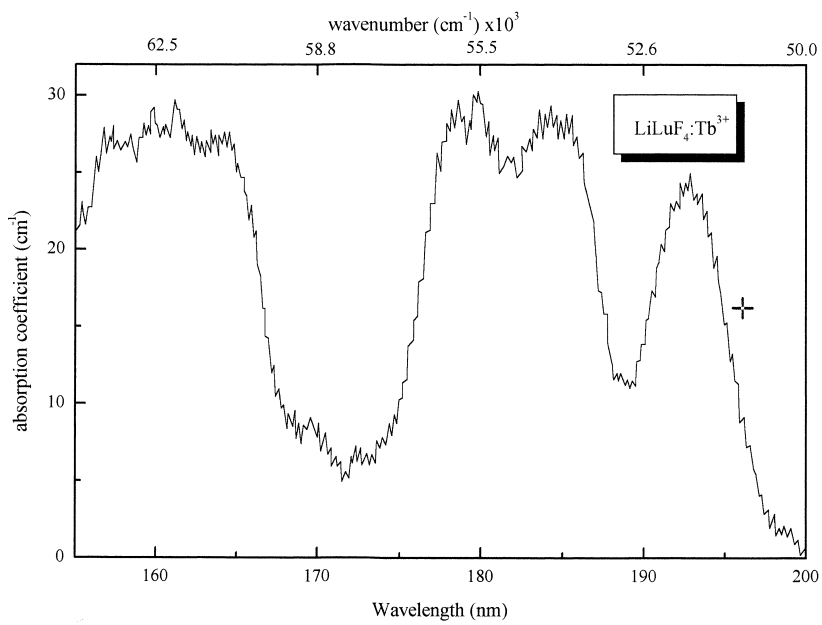

Fig. 3. Absorption spectrum of the $LiLuF_4:Tb^{3+}$ crystal in the spectral range from 155 to 200 nm. The concentration of the Tb^{3+} ion in the $LiLuF_4$ crystal was 0.1 at%, the crystal sample was 0.5 mm thick. The absorption coefficient increases to high values below 155 nm and above 200 nm.

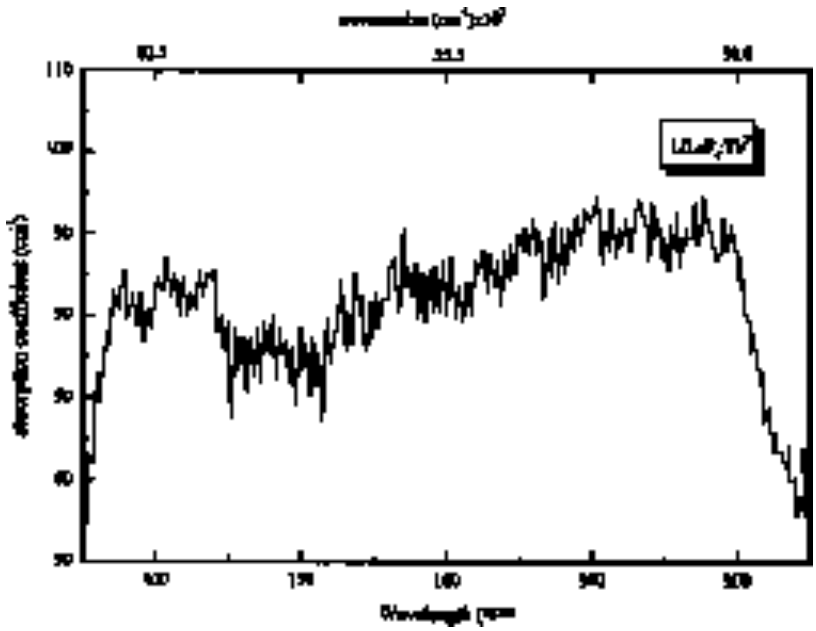

Fig. 4. Absorption spectrum of the $LiLuF_4$:Tb^{3+} crystal in the spectral range from 155 to 200 nm. The concentration of the Tb^{3+} ion in the $LiLuF_4$ crystal was 0.5 at% the crystal sample was 0.2 mm thick. The absorption coefficient increases to high values below 155 nm and above 200 nm.

In order to find the relative energy position of the Stark components, it is necessary to construct the basic functions for the Γ_{1-5} irreducible representations, and then calculate the matrix elements of the electrostatic potential on the Tb^{3+} ion, for each one of the eight Stark components. In this approximation the total angular momentum J, is the good quantum number (J–J coupling). However in order to skip lengthy calculations of the matrix elements of the ligand field of the Tb^{3+} ion, a different approach can be applied considering the orbital angular momentum of the d electron ($L = 2$) as the good quantum number. In this approximation the Γ_4 irreducible representation, has the lowest energy in the tetragonal site symmetry. The next irreducible representation with energy higher than Γ_4, is Γ_5, followed by Γ_3 and Γ_1.

The Γ_2 and the Γ_5 Stark components, are double and triple degenerate, and the degeneracy can be raised when the L–S coupling strength is strong enough within the levels of the $4f^7 5d$ electronic configuration. The splitting of the levels of the $4f^7 5d$ electronic configuration due to the L–S coupling, is only few hundred wavenumbers, and this value is considerably smaller than the crystal field splitting. We assign therefore the triple degenerate Γ_5 Stark component to the energy levels at 54.4×10^3, 55.5×10^3, and 55.9×10^3 cm^{-1}, and the double degenerate Γ_2 Stark component to the energy levels at 62.3×10^3 and 63.3×10^3 cm^{-1} respectively. The remaining three Stark components Γ_1, Γ_3 and Γ_4 were assigned to the energy levels at 67.4×10^3, 52.0×10^3 and 47.0×10^3 cm^{-1} respectively.

3.1.2. 128–140 nm

The next to the lowest ^8S level of the $4f^7 5d$ electronic configuration, is the $4f^7(^6P)5d$ one. The exact value of the separation between the ^6S and the ^6P levels of the $4f^7$ electronic configuration is not known exactly, but it might be assumed to be of the same order of magnitude as in the case of Gd^{3+} ions, which is 32.0×10^3 cm^{-1} [24]. The $4f^7(^6P)5d$ electronic configuration has four terms which are excited from the $^7F_6$ ground level of the $4f^8$ electronic configuration, the $^7F_6$, $^7F_5$, $^7G_7$ and the $^7G_6$. The crystal field splits all these levels to a total number of 26 Stark components for C_{4v} or S_4 site symmetry. However if the selection rules for dipole transitions $\Delta S = 0$, $\Delta l = \pm 1$, $\Delta L = 0, \pm 1$, $\Delta J = 0, \pm 1$ ($J = 0 \rightarrow J = 0$ forbidden) and $\Delta J = \Delta L$ applied only fourteen transitions remain after the excitation from the ground level $^7F_6$ which occupies the spectral region from 120–140 nm, Table 1. Five of the transitions are indicated in the absorption spectrum of Fig. 2. A similar structure has been observed previously for the $LiYF_4$:Tb^{3+} crystal in this spectral range [19].

From the absorption spectrum of Fig. 5, the band gap of the $LiLuF_4$ crystal is 77.6×10^3 cm^{-1} wide (within the experimental error of 350 wavenumbers). It is possible that the levels of the $4f^7 5d$ electronic configuration overlap with the levels of the $4f^7 6s$ electronic configuration below 120 nm [20].

3.2. The LIF spectrum

The laser induced fluorescence spectrum, in the spectral range from 150 to 300 nm, under excitation at 157.6 nm,

Table 1
Crystal field splitting of the $4f^7(^6P)5d$ and $4f^7(^8S)5d$ electronic configurations of the Tb^{3+} ions in the crystal enviroment of tetragonal symmetry

Configuration	Terms	J	ΔL	ΔJ	Dipole transitions $4f^8(^7F_6) \rightarrow 4f^75d$ Level $\Delta L = \Delta J$
$4f^7(^6P)5d$	^7F	5	1	0	–
		6	0	0	$^7F_6$
	^7G	6	−1	−1	$^7G_7$
		7	0	−1	–
$4f^7(^8S)5d$	^7D	5	1	1	$^7D_5$

with the F_2 laser, for 0.01 at% concentration of the Tb^{3+} ion at liquid nitrogen temperature, is shown in Fig. 5. There was no difference between the LIF spectra at room and liquid nitrogen temperatures. The fluorescence peaks were assigned to the dipole transitions between the levels of the $4f^75d$ electronic configuration and the levels of the $4f^8$ electronic configuration of the Tb^{3+} ion. When the Tb^{3+} ion is excited from its $4f^8(^7F_6)$ ground level, to a given level of the $4f^75d$ electronic configuration, our experimental evidence indicates that it populates the levels of the $4f^8$ electronic configuration, when it is deexcited, from both the levels and the edge of the $4f^75d$ electronic configuration. This is due to the fact that after excitation to the levels of the $4f^75d$ electronic configuration, emission takes place at wavelengths shorter than 220 nm, which is the wavelength which corresponds to the transition between the edge of the levels of the $4f^75d$ electronic configuration and the ground level $^7F_6$ of the $4f^8$ electronic configuration, Figs. 5 and 6. This is a rather common response to phonon excitation of the trivalent RE ions in fluoride dielectric crystals, and it has been observed previously for other dielectric crystals doped with RE ions as well. For example, it has been pointed out earlier [21], that at low temperature the excited d levels of Eu, Dy, Er, and the Tb trivalent RE ions relax directly (and from the edge of the band) to the ground level with emission of one VUV or UV photon.

An additional strong experimental evidence, which indicates that the $4f^{n-1}5d$ levels of trivalent RE ions in dielectric fluoride crystals relax to the $4f^n$ levels either

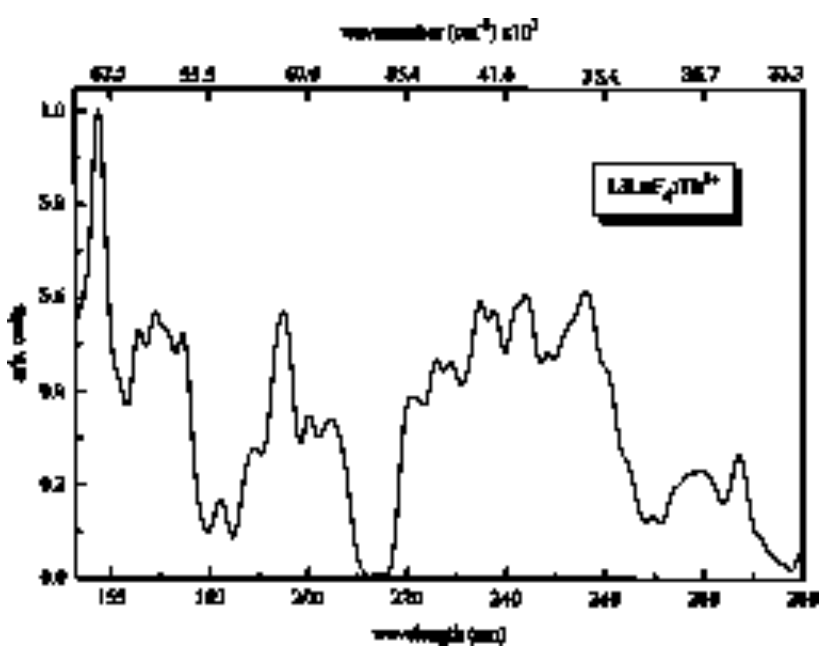

Fig. 5. Laser induced fluorescence spectrum of LiLuF:Tb crystal under the F_2 laser excitation at 157.6 nm in the spectral region from 150 to 300 nm. The concentration of the Tb^{3+} ion in the $LiLuF_4$ crystal was 0.01 at%.

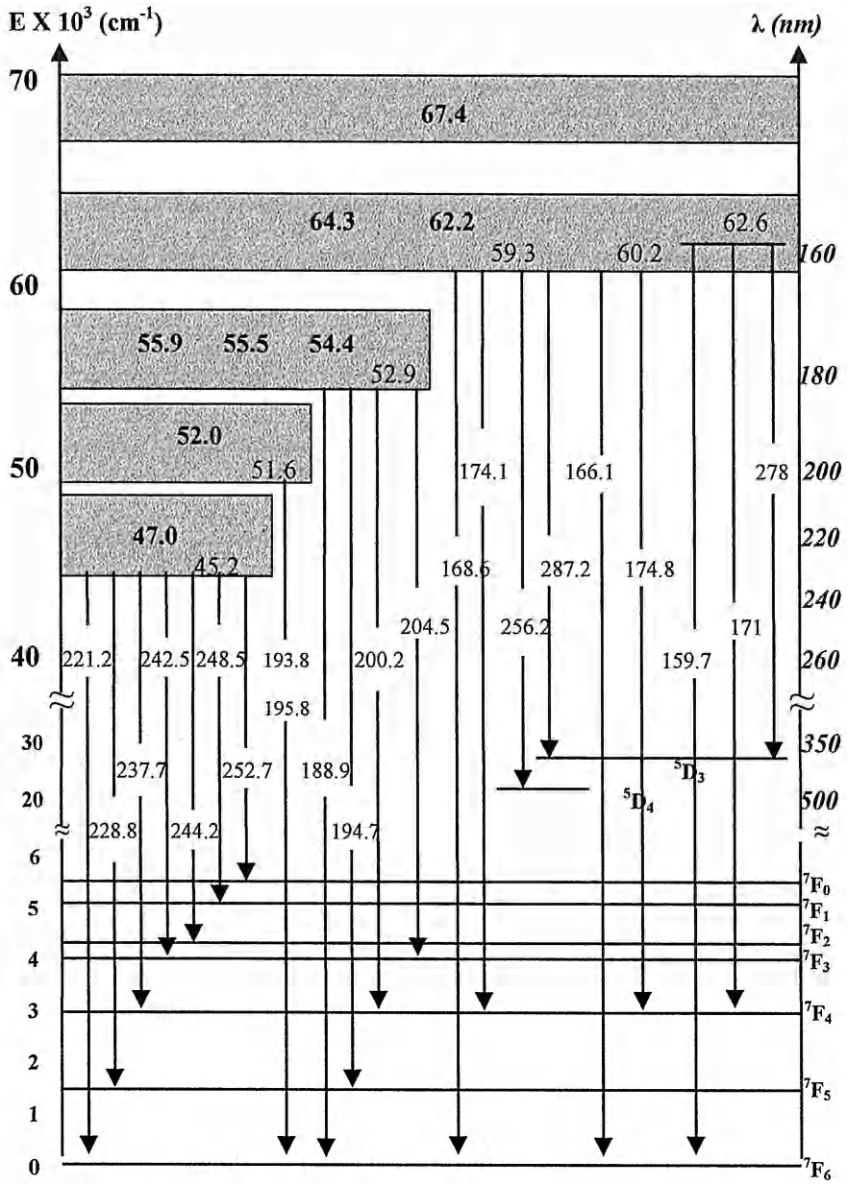

Fig. 6. Simplified energy diagram of the Tb^{3+} ion where the various transitions of the laser induced fluorescence spectra are shown. The position of the levels of the $4f^7 5d$ electronic configuration is where the maximum absorption occurs.

directly, or/and from the edge of the band, is that the emission spectrum, depends on the wavelength of the exciting radiation [25]. To interpret these experimental results let us consider the inter and intraconfigurational transitions and the interaction of the electronic levels with the phonons of the crystal lattice. The $4f^n$ levels are well screened, and usually phonon-assisted lines are not present in the absorption and the emission spectra of the intraconfigurational transitions [24]. The interaction between the $4f^n$ levels and the phonons manifests itself in a different way, namely in radiationless transitions, occurring when two energy levels are separated by less than 1000 cm^{-1}, which is the combined energy of few phonons [24]. As the 5d levels are less well screened, interconfigurational transitions may be assisted by phonons. When a single optically active center absorbs a photon from its ground level of the $4f^8$ electronic configuration, it is excited to the levels of the $4f^7 5d$ electronic configuration. From there competition between radiative and nonradiative transitions starts. The nonradiative transitions are faster and the ion will decay to the lower of the $4f^n 5d$ levels. However in the case of electronic transitions from inside the levels of the $4f^n 5d$

electronic configuration, the emission spectra could be interpreted on the basis of the three following different processes:

1. Formation of optically active RE centres of different site symmetry, which might be present at high concentration of RE ions.
2. Direct $4f^7 5d \rightarrow 4f^8$ emission from the levels of the $4f^7 5d$ electronic configuration.
3. Emission from the levels of the $4f^7 5d$ electronic configuration due to repopulation of these levels.

Regarding the formation of optically active RE centres of different site symmetry, the absorption spectra at various concentrations of the RE ion, Figs. 2, 3, 4, suggest the presence of only one type of symmetry for the RE ion, for low concentration of Tb^{3+} ions, in agreement with Ref. [24].

On the other hand, direct emission from the levels of the $4f^7 5d$ electronic configuration could take place only when two successive electronic levels are well separated by the combined energy of few phonons as it was mentioned previously. However according to Szczurek and Schlesinger [24], there are 3106 electronic levels of the $4f^7 5d$ electronic configuration in the energy range from 80.0×10^3 to 45.0×10^3 cm^{-1}, and this number corresponds to the energy level density of 13 electronic levels per wavenumber (considering an even distribution of the energy levels over the spectral range). Hence there is a small probability for direct transitions between the Stark components of the levels of the $4f^7 5d$ electronic configuration and the levels of the $4f^8$ electronic configuration. Therefore the LIF spectrum can be interpreted provided that the third process of repopulation of the levels of the $4f^7 5d$ electronic configuration is taking place. Repopulation occurs via phonon reabsorption and trapping within the levels of the $4f^7 5d$ electronic configuration. These kind of processes have their origin in strong ionic coupling, between two different Tb^{3+} ions through multipole or exchange interactions, and they have been observed previously for different crystal samples as well [26]. In fact, this effect has been observed as early as 1941 by Van Vleck [27] and recently it was reported for excited states of ruby as well by Geschwind et al. [28]. They observed trapping of phonons, which are resonant with the E and 2A excited states. Experiments with Cr^{3+} ions were carried out as well by Dijkhuis et al. [29]. In these experiments it was observed that when the population of the excited E level is low, the phonons decay to the thermal reservoir. However when the population of the E level is large, the phonon produced by the $2A \rightarrow E$ transitions at one ionic site, is quickly trapped by another Cr^{3+} site in the E state, the latter being excited to the 2A state after absorption of the phonon. The repopulating process will cease when the trapped phonons escape from the active volume by frequency shifting via the interconfigurational transitions. Phonon trapping is usually detected by observing the fluorescent radiation from the excited levels to the ground state in experimental conditions similar to ours. In the case of weak electron $[4f^{n-1}]$–phonon interaction and/or spin forbidden $4f^{n-1}5d$ transitions, the phonon trapping and the reabsorption processes compete with the non-radiative relaxation process within the levels of the $4f^{n-1}5d$ electronic configuration. In this case, the interconfigurational transitions from inside the levels of the $4f^{n-1}5d$ electronic configuration are strong enough, as for example in the case of Tb^{3+}, Gd^{3+} and Er^{3+} ions [16,18,30]. In the case of strong electron–phonon interaction, as for example for the Nd^{3+} ion, the rate of the internal relaxation within the levels of the $4f^{n-1}5d$ electronic configuration is higher than the rate of the phonon reabsorption within the levels of the $4f^{n-1}5d$ electronic configuration. In this case the dipole transitions originate mainly from the edge of the levels of the $4f^{n-1}5d$ electronic configuration [30,31].

As one can find from the LIF spectrum of Fig. 5, the dipole transitions, between the $^7D_5$ Stark components of the $4f^7 5d$ electronic configuration and the levels of the $4f^8$ electronic configuration, are due to the dipole transitions $^7D_5 \rightarrow {}^7F_{4,5,6}$, which satisfy the selection rules for dipole transitions $\Delta S = 0$, $\Delta l = +1, -1$, $\Delta L = 0, +1, -1$, $\Delta J = 0, +1, -1$ and $\Delta J = \Delta L$, Table 1.

3.2.1. 220–253 nm

The emission band, which covers the spectral range from 220 to 253 nm, reflects the wide electronic character of the $4f^7 5d(^7D_5) \rightarrow 4f^8(^7F_{0-6})$ dipole transitions of the Γ_4 Stark component of the levels of the $4f^7 5d(^7D_5)$ electronic configuration. The interconfigurational transitions in this spectral range originate from the edge of the levels of the $4f^7 5d$ electronic configuration. From the LIF spectrum of Fig. 5, it was found that the energy position with the higher Franck–Condon factor is at $45.2 \pm 0.2 \times 10^3$ cm^{-1}. In this case the following assignments can be made regarding the observed dipole transitions, Fig. 6,

$$4f^7 5d\left[{}^7D_5(\Gamma_4), 45.2 \times 10^3\ cm^{-1}\right] \rightarrow 4f^8\left({}^7F_6, 0\right) + h\nu(221.2\ nm),$$

$$4f^7 5d\left[{}^7D_5(\Gamma_4), 45.2 \times 10^3\ cm^{-1}\right] \rightarrow 4f^8\left({}^7F_5, 1.5 \times 10^3\ cm^{-1}\right) + h\nu(228.8\ nm),$$

$$4f^7 5d\left[{}^7D_5(\Gamma_4), 45.2 \times 10^3\ cm^{-1}\right] \rightarrow 4f^8\left({}^7F_4, 3.1 \times 10^3\ cm^{-1}\right) + h\nu(237.7\ nm).$$

Besides the above observed dipole allowed transitions, dipole-forbidden transitions [32] ($\Delta J \neq 0, \pm 1$) were ob-

served as well from the Γ_4 Stark component of the levels of the $4f^7 5d(^7D_5)$ electronic configuration,

$$4f^7 5d\left[{}^7D_5(\Gamma_4), 45.2\times10^3\ \mathrm{cm}^{-1}\right] \rightarrow 4f^8\left({}^7F_3, 4.0\times10^3\ \mathrm{cm}^{-1}\right) + h\nu(242.5\ \mathrm{nm}),$$

$$4f^7 5d\left[{}^7D_5(\Gamma_4), 45.2\times10^3\ \mathrm{cm}^{-1}\right] \rightarrow 4f^8\left({}^7F_2, 4.2\times10^3\ \mathrm{cm}^{-1}\right) + h\nu(244.2\ \mathrm{nm}),$$

$$4f^7 5d\left[{}^7D_5(\Gamma_4), 45.2\times10^3\ \mathrm{cm}^{-1}\right] \rightarrow 4f^8\left({}^7F_1, 5.0\times10^3\ \mathrm{cm}^{-1}\right) + h\nu(248.5\ \mathrm{nm}),$$

$$4f^7 5d\left[{}^7D_5(\Gamma_4), 45.2\times10^3\ \mathrm{cm}^{-1}\right] \rightarrow 4f^8\left({}^7F_0, 5.6\times10^3\ \mathrm{cm}^{-1}\right) + h\nu(252.7\ \mathrm{nm}).$$

The position of the levels of the $4f^8$ electronic configuration of the Tb^{3+} ion in the $LiLuF_4$ single crystal host is not known exactly. The position of these levels in the free ion case, for the ${}^7F_{0-5}$ terms is at 5.8×10^3, 5.1×10^3, 4.8×10^3, 4.0×10^3, 3.1×10^3, 1.9×10^3 cm^{-1} respectively. From the LIF spectrum of Fig. 5 and for the Γ_4 Stark component, the experimental position of the ${}^7F_{0-5}$ terms in the $LiLuF_4$ crystal was found to be at 5.6×10^3, 5.0×10^3, 4.2×10^3, 4.0×10^3, 3.1×10^3 and 1.5×10^3 cm^{-1} respectively, Table 2. Taking into consideration the fact that the electrons of the $4f^8$ electronic configuration are well screened by the electrons of the 5d electronic configuration, the position of the levels of the $4f^8$ electronic configuration inside the $LiLuF_4$ crystal should be shifted relatively to the position of the levels in the free ion case, by few wavenumbers, and this situation is reflected well in our experimental data.

Table 2
Energy position of the $4f^8$ $({}^7F_{0-5})$ levels of the Tb^{3+} ion in the $LiLuF_4$ crystal host. The energy of the $4f^8$ $({}^7F_{0-5})$ levels was fitted to the experimental values taken from the LIF spectrum in the spectral regions from 220 to 235 and 193 to 220 nm respectively

Term $4f^8$	Free ion E_c ($\times10^3$ cm^{-1})	$LiLuF_4$	
		220–235 nm E_c ($\times10^3$ cm^{-1}) Γ_4	190–220 nm E_c ($\times10^3$ cm^{-1}) Γ_5
${}^7F_6$	0	0	0
${}^7F_5$	1.9	1.5	1.5
${}^7F_4$	3.1	3.1	3.0
${}^7F_3$	4.0	4.0	4.0
${}^7F_2$	4.8	4.2	–
${}^7F_1$	5.1	5.0	–
${}^7F_0$	5.8	5.6	–

3.2.2. 193–220 nm

Similarly the emission spectrum which covers the spectral region from 193 to 220 nm, can be assigned to the dipole transitions between the Γ_5 Stark component of the $4f^7 5d({}^7D_5)$ electronic configuration, with maximum absorption at 54.4×10^3 cm^{-1} and the levels of the $4f^8$ electronic configuration. In this case the Franck–Condon factor of the corresponding transitions, has its highest value at $52.9\pm0.2\times10^3$ cm^{-1}. For these transitions the following assignments can be made within the limits of the experimental error of 200 cm^{-1} for these wavelengths,

$$4f^7 5d\left[{}^7D_5(\Gamma_5), 52.9\times10^3\ \mathrm{cm}^{-1}\right] \rightarrow 4f^8\left({}^7F_6\right) + h\nu(188.9\ \mathrm{nm}),$$

$$4f^7 5d\left[{}^7D_5(\Gamma_5), 52.9\times10^3\ \mathrm{cm}^{-1}\right] \rightarrow 4f^8\left({}^7F_5, 1.5\times10^3\ \mathrm{cm}^{-1}\right) + h\nu(194.7\ \mathrm{nm}),$$

$$4f^7 5d\left[{}^7D_5(\Gamma_5), 52.9\times10^3\ \mathrm{cm}^{-1}\right] \rightarrow 4f^8\left({}^7F_4, 3.0\times10^3\ \mathrm{cm}^{-1}\right) + h\nu(200.2\ \mathrm{nm}),$$

$$4f^7 5d\left[{}^7D_5(\Gamma_5), 52.9\times10^3\ \mathrm{cm}^{-1}\right] \rightarrow 4f^8\left({}^7F_3, 4.0\times10^3\ \mathrm{cm}^{-1}\right) + h\nu(204.5\ \mathrm{nm}).$$

From the LIF spectrum of Fig. 5, it was found that the position of the Stark components of the levels of the $4f^8$ electronic configuration ${}^7F_{3-5}$ in the $LiLuF_4$ crystal is at 4.0×10^3, 3.0×10^3 and 1.5×10^3 cm^{-1} respectively, Table 2, in agreement with the energy position of these levels in the spectral range from 220 to 253 nm.

The transition around 194 nm could originate as well from the Γ_3 Stark component with maximum absorption at 52.0×10^3 cm^{-1} at 51.6×10^3 cm^{-1},

$$4f^7 5d\left[{}^7D_5(\Gamma_3), 51.6\times10^3\ \mathrm{cm}^{-1}\right] \rightarrow 4f^8\left({}^7F_6\right) + h\nu(193.8-194.7\ \mathrm{nm}).$$

3.2.3. 159–175 nm

The emission spectrum which covers the spectral range from 159 to 174 nm, can be assigned to the dipole transitions between the Γ_2 Stark component of the $4f^7 5d({}^7D_5)$ electronic configuration, and the levels of the $4f^8$ electronic configuration. However, for this spectral range, it is difficult to make any specific assignment for the $4f^7 5d \rightarrow 4f^8$ transitions, due to the presence of intense scattered laser light. Taking into consideration the position of the levels of the Tb^{3+} ions of the $4f^8$ electronic configuration in the $LiLuF_4$ crystal host, Tables 1, 2, and

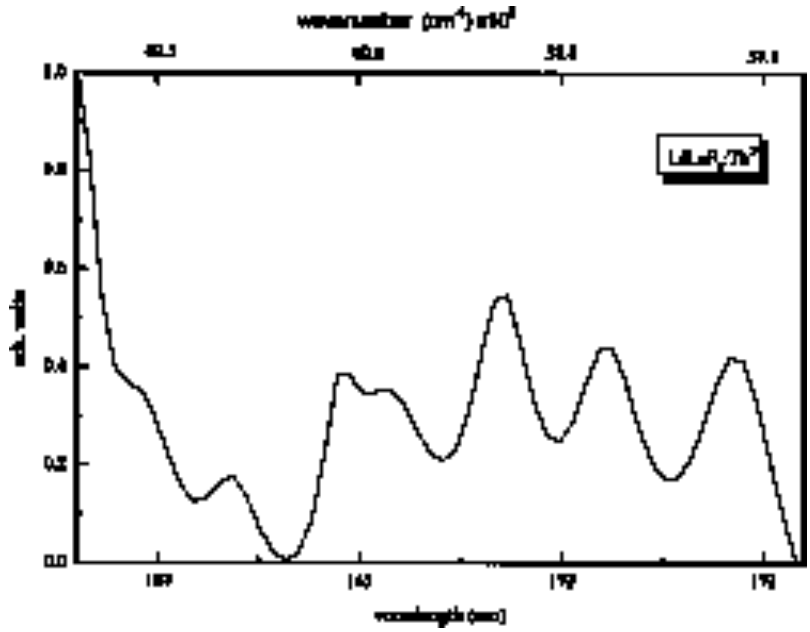

Fig. 7. Laser induced fluorescence spectrum of LiLuF:Tb crystal under the F_2 laser excitation at 157.6 nm in the spectral region from 157 to 175 nm. The concentration of the Tb^{3+} ion in the $LiLuF_4$ crystal was 0.01 at%.

the emission spectrum of Fig. 7, the following assignments can be made for the $4f^75d \rightarrow 4f^8$ transitions:

$$4f^75d\left[{}^7D_5(\Gamma_5), 62.6\times10^3\,cm^{-1}\right] \rightarrow 4f^8\left({}^7F_6\right) + h\nu(159.7\,nm),$$

$$4f^75d\left[{}^7D_5(\Gamma_2), 62.6\times10^3\,cm^{-1}\right] \rightarrow 4f^8\left({}^7F_4 \text{ or } {}^7F_3\right) + h\nu(171\,nm),$$

$$4f^75d\left[{}^7D_5(\Gamma_2), 59.3\times10^3\,cm^{-1}\right] \rightarrow 4f^8\left({}^7F_6\right) + h\nu(168.6\,nm),$$

$$4f^75d\left[{}^7D_5(\Gamma_2), 59.3\times10^3\,cm^{-1}\right] \rightarrow 4f^8\left({}^7F_4\right) + h\nu(174.1\,nm).$$

The transitions at 278, 256.2 and 287.2 nm were assigned to spin-forbidden transitions [32], taking into consideration that the energy position of the $^5D_4$ and $^5D_3$ levels of the $4f^8$ electronic configuration in the free Tb^{3+} ion case, is at 20.5×10^3 and 26.0×10^3 cm^{-1} respectively.

$$4f^75d\left[{}^7D_5(\Gamma_1), 62.6\times10^3\,cm^{-1}\right] \rightarrow 4f^8\left({}^5D_3\right) + h\nu(278\,nm),$$

$$4f^75d\left[{}^7D_5(\Gamma_2), 59.3\times10^3\,cm^{-1}\right] \rightarrow 4f^8\left({}^5D_4\right) + h\nu(256.2\,nm),$$

$$4f^75d\left[{}^7D_5(\Gamma_2), 59.3\times10^3\,cm^{-1}\right] \rightarrow 4f^8\left({}^5D_3\right) + h\nu(287.2\,nm).$$

The transitions at 166.1 and 174.8 nm, Fig. 7 can be assigned to interconfigurational transitions which originate from the energy position at 60.2×10^3 cm^{-1},

$$4f^75d\left[{}^7D_5(\Gamma_2), 60.2\times10^3\,cm^{-1}\right] \rightarrow 4f^8\left({}^7F_6\right) + h\nu(166.1\,nm),$$

$$4f^75d\left[{}^7D_5(\Gamma_2), 60.2\times10^3\,cm^{-1}\right] \rightarrow 4f^8\left({}^7F_4\right) + h\nu(174.8\,nm).$$

4. Conclusions

LIF and absorption spectra of $LiLuF_4$:Tb^{3+} crystals have been obtained in the VUV and UV regions of the spectrum. We observed eight and five dipole transitions of the Tb^{3+} ion in $LiLuF_4$ crystals, between the $^7F_6$ ground level of the $4f^8$ electronic configuration and the Stark components of the levels of the $4f^7(^8S)5d$ and the $4f^7(^6P)5d$ electronic configurations respectively. The LIF spectrum can be interpreted provided that the $4f^75d \rightarrow 4f^8$ dipole transitions originate from the Stark components of the $^2D_5$ level of the $4f^7(^8S)5d$ electronic configuration. This is a consequence of phonon trapping and phonon reabsorption within the levels of the $4f^75d$ electronic configuration.

Acknowledgements

The authors acknowledge financial support from NATO (Linkage grant no. 931595) for R.Yu Abdulsabirov, V.V.

Semashko, A.K. Naumov and S. Korableva. We also acknowledge stimulating discussions with Dr. T. Szczurek of the Torun University, during his visit to Athens.

References

[1] R.W. Waynant, P.H. Klein, Appl. Phys. Lett. 46 (1985) 1.
[2] M.A. Dubinskii, A.C. Cefalas, C.A. Nicolaides, Optics Comm. 88 (1992) 122.
[3] M.A. Dubinskii, V.V. Semashko, A.K. Naumov, R.Yu. Abdulsabirov, S.L. Korableva, J. Mod. Optics 40 (1993) 1.
[4] C.D. Marshall, J.A. Speth, S.A. Payne, W.F. Krupke, G.J. Quarles, V. Castillo, J. Opt. Soc. Am. B 11 (1994) 2054.
[5] M.J.F. Digonnet, R.W. Sadowski, H.J. Shaw, R.H. Pantell, Opt. Fiber Technol. 3 (1997) 44.
[6] K.S. Syed, G.J. Crofts, M.J. Damjen, J. Opt. Soc. Am. B 13 (1997) 1892.
[7] C.M. Combes, P. Dorenbos, C.W.E. Vaneijk, C. Pedrini, H.W. Denmartog, J.Y. Gesland, P.A. Rodnyi, J. Lumin. 71 (1997) 65.
[8] S. Kubodera, M. Kitahara, J. Kawanaka, W. Sasaki, K. Kurosawa, Appl. Phys. Lett. 69 (1996) 452.
[9] J.C. Krupa, I. Gerard, A. Mayolet, P. Martin, Acta Phisica Polonika A 84 (1993) 843.
[10] A.M. Srivastava, S.J. Duclos, Chem. Phys. Lett. 275 (1997) 453.
[11] J. Thogersen, J.D. Gill, H.K. Haugen, Optics Comm. 132 (1996) 83.
[12] G.E. Venikouas, G.J. Quarles, J.P. King, R.C. Powell, Phys. Rev. B 30 (1984) 2401.
[13] J.L. Adam, W.A. Silbey, D.R. Gabbe, J. Lumin. 33 (1985) 391.
[14] M. Dulick, G.E. Faulkner, N.J. Cockroft, D.C. Nguyen, J. Lumin. 48/49 (1991) 517.
[15] A.A. Ellens, H. Andres, M.L.H. ter Heerdt, R.T. Wegt, A. Meijerink, G. Blasse, Phys. Rev. B 55 (1997) 180.
[16] A.A. Ellens, H. Andres, M.L.H. ter Heerdt, R.T. Wegt, A. Meijerink, G. Blasse, Phys. Rev. B 55 (1997) 173.
[17] R.T. Wegh, H. Donker, A. Meijerink, Phys. Rev. B 57 (1998) 2025.
[18] R.T. Wegh, H. Donker, A. Maijerink, R.J. Lamminmaki, J. Holsa, Phys. Rev. B 56 (1997) 13841.
[19] E. Sarantopoulou, A.C. Cefalas, M.A. Dubinskii, Z. Kollia, C.A. Nicolaides, R.Y. Abdulsabirov, S.L. Korableva, A.K. Naumov, V.V. Semashko, J. Mod. Optics 41 (1994) 767.
[20] Wm.S. Heaps, L.R. Elias, W.M. Yen, Phys. Rev. B 13 (1976) 94.
[21] J.C. Krupa, I. Gerard, A. Mayolet, P. Martin, Acta Physica Polonika A 84 (1993) 843.
[22] A.A. Kaminskii, Phys. Stat. Sol. (a) 97 (1986) k53.
[23] G.H. Dieke, H.M. Crosswhite, Appl. Optics 2 (1963) 675.
[24] T. Szczurek, Schlesinger, in: B. Jezowska-Trezbiatowska, J. Legendriewicz, W. Streak (Eds.), Rare Earth Spectroscopy, World Scientific, Singapore, 1985, p. 309, and references therein.
[25] K.M. Devyatkova, O.N. Ivanova, S.A. Oganesyan, K.B. Seiranyan, S.P. Chernov, Sov. Phys. Dolk. 35 (1990) 577.
[26] W.M. Yen, P.M. Selzer (Eds.), Laser Spectroscopy of Solids, Springer, Berlin, 1981.
[27] J.H. Van Vleck, Phys. Rev. 59 (1941) 724.
[28] S. Geschwind, G.E. Devlin, R.L. Cohen, S.L. Chinn, Phys. Rev. A 137 (1965) 1087.
[29] J.I. Dijkhuis, A. Van der Pol, H.W. de Wijn, Phys. Rev. Lett. 37 (1976) 1554.
[30] E. Sarantopoulou, Z. Kollia, A.C. Cefalas, M.A. Dubinskii, C.A. Nicolaides, R.Y. Abdulsabirov, S.L. Korableva, A.K. Naumov, V.V. Semashko, Appl. Phys. Lett. 65 (1994) 813.
[31] E. Sarantopoulou, A.C. Cefalas, M.A. Dubinskii, C.A. Nicolaides, R.Y. Abdulsabirov, S.L. Korableva, A.K. Naumov, V.V. Semashko, Optics Lett. 19 (1994) 499.
[32] T. Hoshina, S. Kuboniwa, J. Phys. Soc. Japan 31 (1971) 828.